GaAs(001) Surface under Conditions of Low As Pressure: Evidence for a Novel Surface Geometry

Sung-Hoon Lee,[1] Wolfgang Moritz,[2] and Matthias Scheffler[1]

[1]*Fritz-Haber-Institut der Max-Planck-Gesellschaft, Faradayweg 4-6, D-14195 Berlin, Germany*

[2]*Institut für Kristallographie und Angewandte Mineralogie, Universität München, Theresienstrasse 41, D-80333 München, Germany*

(Received 19 April 2000)

Using density-functional theory we identify a new low-energy structure for GaAs(001) in an As-poor environment. The discovered geometry is qualitatively different from the usual surface-dimer based reconstructions of III-V semiconductor (001) surfaces. The stability of the new structure, which has a $c(8 \times 2)$ periodicity, is explained in terms of bond saturation and favorable electrostatic interactions between surface atoms. Simulated scanning tunneling microscopy images are in good agreement with experimental data, and a low-energy electron diffraction analysis supports the theoretical prediction.

PACS numbers: 68.35.Bs, 61.14.Hg, 68.35.Md, 73.20.At

III-V semiconductors play an increasing role in microelectronics, such as light-emitting diodes and high frequency, low noise devices for mobile phones, and are important candidates for the development of devices in the emerging field of spin electronics. The knowledge of the surface atomic structure is a prerequisite to achieve understanding and controlling of the surface or interface electronic properties. As we will show below, however, up to date analyses of surface structures of III-V semiconductors are hindered by some prejudice on the type of structures considered. For an example of the GaAs(001) surface, we show the existence of a new type of surface reconstruction.

The bulk-truncated (001) surface of zinc-blende III-V semiconductors (e.g., GaAs) has two dangling orbitals for each surface atom and therefore is energetically unfavorable. As a consequence, the surface exchanges atoms with the environmental gas phase, altering the surface stoichiometry, and the surface atoms displace to assume a more favorable bonding geometry [1]. The resulting surface structure depends on the environment, i.e., the As partial pressure and temperature. As-rich conditions have attracted much attention in recent years, and several distinct geometries are known to exist. The so-called $\beta 2$ structure, which has a (2×4) periodicity, has been safely identified [2]: This is the most important surface under As-rich conditions; its unit cell is built from two As dimers followed by two missing dimers [cf. the $\beta 2(4 \times 2)$ structure in the middle column of Fig. 1, but exchange Ga and As atoms]. Recently, conditions with low As partial pressure became important, because the resulting surface stoichiometry is Ga rich and preferable for the deposition of iron and cobalt [3], which can play a role in the nanotechnology of magnetic materials and spin electronics [4].

Most of the known atomic geometries of the III-V (001) surfaces are characterized by the formation of surface dimers. These reconstructions, realized by only a small change of bond angles of surface atoms, are energetically favorable because they reduce the number of dangling orbitals [1,5]. Two known exceptions to this "rule" are the mixed-dimer structure for InP(001) [6,7] and the tetramer structure for GaN(001) [8], but also for these systems the reconstruction is achieved by simply changing bond angles of surface atoms (though for the former system a top-layer P atom is replaced by an In atom). In this Letter, we show that the $c(8 \times 2)$ reconstruction of GaAs(001), observed for As-poor conditions, involves a qualitatively different mechanism to stabilize the surface. This mechanism has not been considered before and is likely to occur at other III-V (001) surfaces as well.

Up to now the $c(8 \times 2)$ surface is believed to consist of $\beta 2(4 \times 2)$ subunits (see Fig. 1, middle column). There are Ga-dimer hills and trenches of 4 missing Ga and 2 missing As atoms per (4×2) cell. At the bottom of the trenches the Ga atoms are also dimerized. The $c(8 \times 2)$ surface has been studied by density-functional theory (DFT) [9] and by scanning tunneling microscopy (STM) [10,11]. All these studies support the $\beta 2$-based model, which is also plausible in view of the knowledge

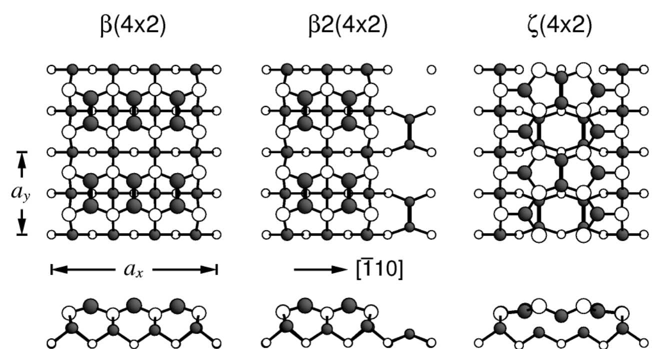

FIG. 1. Top views (upper row) and side views (lower row) of the β, $\beta 2$, and ζ structures of Ga-rich (4×2) surface geometries of the (001) surfaces of III-V semiconductors. The top views display two (4×2) cells. The $c(8 \times 2)$ surface is obtained by repeating the shown cell in the x direction ($[\bar{1}10]$), but shifted by $a_y/2$ in the y direction ([110]). Solid spheres denote Ga atoms and open spheres As atoms. The sphere sizes reflect the distance from the surface. Dimer bonds are marked by thicker lines.

 0031-9007/00/85(18)/3890(4)$15.00 © 2000 The American Physical Society

about As-rich surfaces. Nevertheless, to our estimation the structure identification of the $c(8 \times 2)$ surface is not fully convincing: The interpretation of the STM images is not irrefutable, neither for the filled-states [12,13] nor for the empty-states images [14], and moreover the reliability factor of a low-energy electron diffraction (LEED) analysis was $\frac{1}{2}(R_P + R_{DE}) = 0.58$ [15], which we do not consider decisive.

The $c(8 \times 2)$ surface of GaAs(001) is built from (4×2) units, but the energy gain due to the period doubling is minor [e.g., for the $\beta2$ structure it is less than 0.01 eV per (4×2) cell]. Therefore we performed DFT calculations for various structural models of GaAs(001) with a (4×2) periodicity. The results identify a novel surface geometry as the lowest-energy structure. The new surface structure has two Ga dimers *in the second layer,* which are covered by a nearly planar atomic layer consisting of sp^2-bonded Ga atoms, sp^3-bonded As atoms, and a Ga dimer (see Fig. 1, right column). The DFT calculations show that this $\zeta(4 \times 2)$ surface structure is energetically more favorable than all previously proposed models. Its stability is found to be actuated by the electron counting rule [16,17] (ECR), i.e., the filling of all As dangling orbitals and emptying of all Ga dangling orbitals, and a favorable electrostatic (Ewald) interaction between surface atoms. Simulated STM images and a LEED analysis support this new structure identification.

Our DFT calculations [18] employed the generalized gradient approximation [19] and norm-conserving pseudopotentials [20,21]. The surface is modeled by a periodic slab geometry. Each slab contains 7 or 8 atomic layers and the bottom As layer is passivated by pseudohydrogen atoms [22]. The thickness of the vacuum region is $\sim$9 Å. The electronic wave functions are expanded in a plane-wave basis set with a cutoff energy of 10 Ry. The **k**-space integration is performed with a mesh corresponding to 64 **k** points in the (1×1) surface Brillouin zone. In the course of structure optimization, we allow all the atoms to relax except for the bottom As layer. All above technical parameters were carefully tested to ensure that the numerical accuracy of the below discussed energy differences is better than 0.1 eV per (4×2) cell.

The top surface layer of the $\zeta(4 \times 2)$ structure contains 6 Ga and 8 As atoms per surface unit cell (cf. Fig. 1). Nevertheless, this structure represents a Ga-rich surface termination. Interestingly, from the 8 subsurface Ga atoms, 4 engage into dimers. And from the 14 Ga and As atoms in the top surface layer only two Ga atoms are found to dimerize. The formation of the new geometry can be understood by starting from the β structure (see Fig. 1, left column) that has three Ga dimers and one missing Ga dimer. The $\zeta(4 \times 2)$ structure results when the center Ga dimer of the β structure, together with its four second-layer As atoms, is shifted by $a_y/4$ along the y direction. This translation forces the side Ga dimers to split into sp^2 planar bonding Ga atoms, and also the Ga atoms in the second Ga layer, which are bonded to the moved surface As atoms, now attain a threefold coordination. As a consequence these second-layer Ga atoms form dimers, breaking the bonds with the surface As atoms. The As atoms then move up directing the broken bonds toward the vacuum region, and the center Ga dimer moves down for the As atoms to assume a nearly tetrahedral bonding geometry. This ζ structure exhibits 8 As and 4 Ga dangling orbitals (i.e., the p_z states of the sp^2-bonded Ga atoms) on the top surface layer, and there are 6 Ga dangling orbitals beneath the surface. Thus, from the vacuum side the surface looks as if it were As rich. But in contrast to true As-rich conditions the As surface atoms do not dimerize, which gives the surface a significantly different electronic structure and chemical activity. Counting the coordination, dangling orbitals, and the number of valence electrons (five for each As and three for each Ga atom) yields that in the ζ structure all As dangling orbitals are filled and all Ga dangling orbitals are empty. Thus, the ECR is fulfilled and it is understood that the surface is semiconducting. We also note that per (4×2) cell the ζ structure contains two GaAs pairs more than the $\beta2$ structure, which is the so far believed surface termination.

Our DFT calculations show that the ζ reconstruction has 3.3 meV/Å^2 lower energy than the $\beta2$ structure. Thus, per (4×2) cell ($A = 134$ Å^2) the energy difference ($\Delta E = 0.44$ eV) is significant. In Fig. 2 the calculated surface energies show that the $\zeta(4 \times 2)$ structure is indeed the stable phase in a rather wide range of the As chemical potential at the Ga-rich side. Two points are worth noting. First, the diagram reproduces previous DFT results [9,23], and it shows a new feature: The $\alpha2(2 \times 4)$ structural model suggested for the InAs(001) surface [24] is more stable than the $\beta2(4 \times 2)$ model in the whole allowed range of the As chemical potential, which provides additional evidence against the $\beta2(4 \times 2)$ structure of being a stable phase. Second, the (2×4) counterpart of the $\zeta(4 \times 2)$

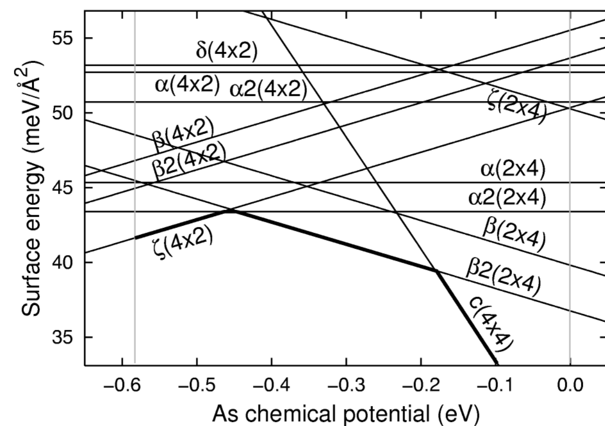

FIG. 2. Surface energies for GaAs(001) surface terminations as a function of the As chemical potential. The thermodynamically allowed range is between −0.58 eV (Ga-rich) and 0.0 eV (As-rich). For figures of the geometries, we refer to Ref. [9], except for the δ and $\alpha2$ structural models that were suggested in Refs. [12] and [24], respectively.

structure is energetically very unfavorable compared to its surface-dimerized version, the $\beta(2 \times 4)$ geometry. This is understood from that in the $\zeta(2 \times 4)$ structure the dangling orbitals of the second-layer As dimers have to be filled: The resulting bonds between the As dimers and the first-layer Ga atoms impose strong strain on the bonding geometry (see also below).

The ECR holds for all three structures: β, $\beta2$, and ζ. The high stability of the latter can be traced back to a more favorable electrostatic interaction between surface atoms. Because all Ga dangling orbitals are empty and As dangling orbitals are full, the electrostatic interaction between Ga and As atoms at the surface is different from that in the bulk. To estimate the significance of the electrostatic interaction, we calculated the Madelung energy for the periodic array of atomic charges at the surface (the charge of Ga atoms in dimers is set $+1/2$, and that of all other atoms is set $\pm 3/4$), divided by the static dielectric constant of GaAs, following an earlier approach of Northrup and Froyen [9]. The calculated Madelung energies are -0.17, -0.67, and -1.57 eV per (4×2) cell for the β, $\beta2$, and ζ models, respectively. Thus, electrostatically the ζ geometry is clearly favored. (On the other hand, the $\zeta(2 \times 4)$ structure has a Madelung energy of only -0.27 eV, which partly explains its contrasting stability.)

We now discuss the experimental support for the ζ structure. For this purpose, we calculated constant-current STM images for various bias voltages using the Tersoff-Hamann approach [25] (see Fig. 3). The low-bias filled-state image ($V_b = -0.4$ V) shows bright double rows running in the y direction ([110]) and gray protrusions in between. The bright row consists of individual features spaced almost equally by $a_y/2$ in the y direction. The gray protrusions, bound together by four of them, exhibit a $c(8 \times 2)$ symmetry. All these features are in good agreement with the high-resolution STM images of Xue *et al.* [11] and Skala *et al.* [12]. It has to be noted that the topmost As atoms underlie the gray protrusions and the edge ones the bright rows, while the former is 0.7 Å higher than the latter. This is because the dangling orbitals of the former have higher binding energies than those of the latter. As a consequence, at higher bias voltages the contrast between the bright and gray sites reduces and eventually reverses ($V_b = -1.5$ V). Interestingly, the early STM study of Biegelsen *et al.* [10] showed bright double rows exhibiting a $c(8 \times 2)$ symmetry, which is consistent with the simulated high-bias image. In other words, the ζ structure accounts well for all the existing filled-state STM images and resolves the discrepancies between them due to different bias voltages, or different Fermi-level pinning. It also provides a good explanation for the empty-state STM image [14], in which two bright rows running in the y direction are separated by $\sim a_x/2$ and each of the rows consists of protrusions spaced by a_y. The simulated empty-state image ($V_b = +1.5$ V) indicates that the two bright rows come from the empty p_z states of the sp^2-bonded Ga atoms, and that the observed a_y spacing of protrusions in a row is due to a small difference in the p_z energy level between the two inequivalent sp^2-bonded Ga atoms (cf. $V_b = +1.8$ V).

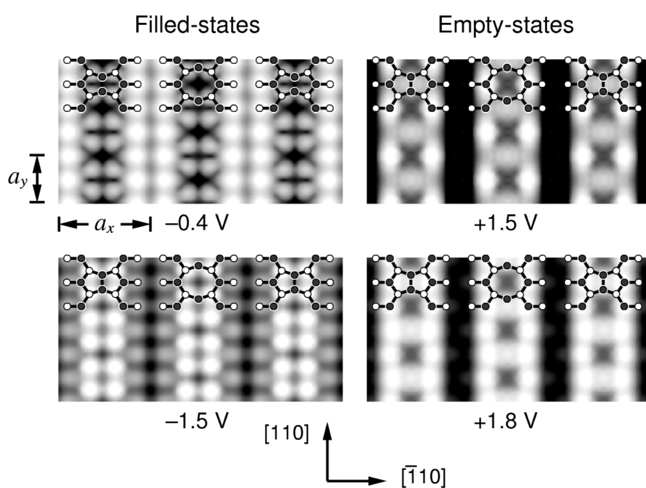

FIG. 3. Simulated STM images of the $c(8 \times 2)$ ζ structure of GaAs(001) for different bias voltages, V_b, which are given with respect to the valence band maximum, E_{VB}. The images map the height of constant electron density [$n(\vec{r}) = 5 \times 10^{-6}$ bohr^{-3}] for the electron density integrated over an energy range between E_{VB} and $E_{VB} + eV_b$. The constant density surface is at 3–4 Å above the atomic surface and has a height corrugation of $\sim$1.5 Å. Full dots mark positions of Ga atoms and open dots mark As atoms.

We further tested the correctness of the ζ structure by performing a LEED analysis. An extensive data set of the $c(8 \times 2)$ reconstruction has been published previously [15], in which a best fit [$\frac{1}{2}(R_P + R_{DE}) = 0.50$] was obtained for the β model. The present LEED calculations were performed using the layer doubling method and a least-squares optimization scheme [26,27]. Up to 12 phase shifts were included depending on the energy. The nonstructural parameters were a constant optical potential of 4.5 eV and an energy dependent real part of the inner potential with $V_0 = 2.8 - 66.0/\sqrt{E + 10.0}$ eV, where E is in eV referring to the muffin tin zero. The parameters for the energy dependency of the inner potential have been fitted to the data. Isotropic thermal vibrations were used for all layers where the temperature factors of the 8 topmost atoms have been optimized while for deeper atoms Debye temperatures of 275 K for Ga and 285 K for As, derived from x-ray measurements [28], were used. Refinement with anisotropic vibrations has not been tried in this analysis. There are in total 16 symmetrically independent atoms in four layers which have been set free in the refinement. This leads to 30 free positional parameters and together with 8 temperature factors and the parameters for the inner potential to a total of 40 free parameters. The data set of Ref. [15] consists of 18 symmetrically independent beams with a total energy range of 2020 eV. In a first step the structure from the DFT calculation was used, and the inner potential, real and imaginary parts, were optimized. Then, the temperature factors in the top layer

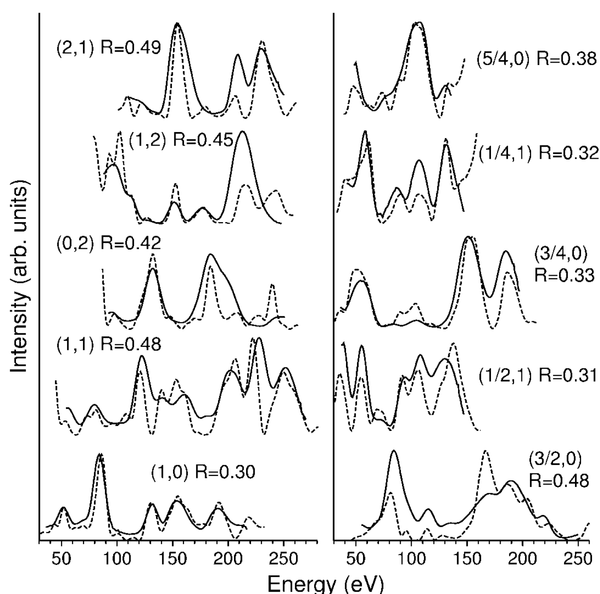

FIG. 4. Comparison between experimental (solid line) and calculated (dashed line) LEED curves for the $c(8 \times 2)$ ζ structure of GaAs(001). The overall R factors are $R_P = 0.39$ and $R_{DE} = 0.38$.

(top 8 atoms) were optimized. The further refinement proceeded in steps, in which z positions, lateral positions, and temperature factors were optimized separately, and in a final step all parameters were set free. The final R-factor is $R_P = 0.39$ and $R_{DE} = 0.38$ (see Fig. 4) which is a significantly better value than that of the previously favored structural model. The $I(V)$ curves show practically all peaks in the right positions. Our LEED analysis yields atomic positions which differ mostly by less than 0.05 Å from those determined by the DFT calculation. The remaining misfit may be attributed to surface defects: The surface, prepared by Ar ion bombardment and annealing, as used in the LEED experiment, exhibits a nearly regular arrangement of surface defects [29].

In conclusion, we have shown that the GaAs(001)-$c(8 \times 2)$ surface is reconstructed with the $\zeta(4 \times 2)$ structural unit. The structure and detailed geometry was found by DFT calculations. The theoretical results were used for simulations of STM images and for a LEED analysis, both of which are compared well with experimental data. We note that this new type of reconstruction has consequences for electronic structures, surface diffusion, and growth processes, and also opens the way to structural models for a number of presently unknown and important semiconductor surface reconstructions.

This work was supported by the Sfb 290 of the Deutsche Forschungsgemeinschaft. S. H. L. acknowledges support from KOSEF and the Alexander von Humboldt Foundation.

[1] Q. K. Xue, T. Hashizume, and T. Sakurai, Prog. Surf. Sci. **56**, 1 (1997).
[2] V. P. LaBella *et al.,* Phys. Rev. Lett. **83**, 2989 (1999).
[3] Y. B. Xu *et al.,* Phys. Rev. B **58**, 890 (1998).
[4] G. A. Prinz, Science **282**, 1660 (1998).
[5] C. B. Duke, Chem. Rev. **96**, 1237 (1996).
[6] C. D. MacPherson *et al.,* Phys. Rev. Lett. **77**, 691 (1996).
[7] W. G. Schmidt *et al.,* Phys. Rev. B **57**, 14 596 (1998).
[8] J. Neugebauer *et al.,* Phys. Rev. Lett. **80**, 3097 (1998).
[9] J. E. Northrup and S. Froyen, Phys. Rev. Lett. **71**, 2276 (1993); Phys. Rev. B **50**, 2015 (1994).
[10] D. K. Biegelsen *et al.,* Phys. Rev. B **41**, 5701 (1990).
[11] Q. K. Xue *et al.,* Phys. Rev. Lett. **74**, 3177 (1995).
[12] S. L. Skala *et al.,* Phys. Rev. B **48**, 9138 (1993).
[13] P. Moriarty *et al.,* J. Vac. Sci. Technol. B **14**, 943 (1996).
[14] Q. K. Xue *et al.,* Thin Solid Films **281–282**, 556 (1996).
[15] J. Cerdá, F. J. Palomares, and F. Soria, Phys. Rev. Lett. **75**, 665 (1995).
[16] W. A. Harrison, J. Vac. Sci. Technol. **16**, 1492 (1979).
[17] M. D. Pashley, Phys. Rev. B **40**, 10 481 (1989).
[18] M. Bockstedte *et al.,* Comput. Phys. Commun. **107**, 187 (1997); http://www.fhi-berlin.mpg.de/th/fhimd/
[19] J. P. Perdew, K. Burke, and M. Ernzerhof, Phys. Rev. Lett. **77**, 3865 (1996).
[20] D. R. Hamann, Phys. Rev. B **40**, 2980 (1989).
[21] M. Fuchs and M. Scheffler, Comput. Phys. Commun. **119**, 67 (1999); http://www.fhi-berlin.mpg.de/th/fhi98md/fhi98PP/
[22] K. Shiraishi, J. Phys. Soc. Jpn. **59**, 3455 (1990).
[23] N. Moll *et al.,* Phys. Rev. B **54**, 8844 (1996).
[24] H. Yamaguchi and Y. Horikoshi, Phys. Rev. B **51**, 9836 (1995).
[25] J. Tersoff and D. R. Hamann, Phys. Rev. B **31**, 805 (1985).
[26] H. Over *et al.,* Surf. Sci. **219**, L637 (1992).
[27] G. Kleinle, W. Moritz, and G. Ertl, Surf. Sci. **238**, 119 (1990).
[28] U. Pietsch and N. K. Hansen, Acta Cryst. B **52**, 596 (1996).
[29] F. Bensch and G. Bayreuther *et al.* (unpublished).